Climate and biogeochemical response to a rapid melting of the West Antarctic Ice Sheet during interglacials and implications for future climate

L. Menviel,[1] A. Timmermann,[2] O. Elison Timm,[2] and A. Mouchet[3]

[1] We study the effects of a massive meltwater discharge from the West Antarctic Ice Sheet (WAIS) during interglacials onto the global climate-carbon cycle system using the Earth system model of intermediate complexity LOVECLIM. Prescribing a meltwater pulse in the Southern Ocean that mimics a rapid disintegration of the WAIS, a substantial cooling of the Southern Ocean is simulated that is accompanied by an equatorward expansion of the sea ice margin and an intensification of the Southern Hemispheric Westerlies. The strong halocline around Antarctica leads to suppression of Antarctic Bottom Water (AABW) formation and to subsurface warming in areas where under present-day conditions AABW is formed. This subsurface warming at depths between 500 and 1500 m leads to a thermal weathering of the WAIS grounding line and provides a positive feedback that accelerates the meltdown of the WAIS. Our model results further demonstrate that in response to the massive expansion of sea ice, marine productivity in the Southern Ocean reduces significantly. A retreat of the WAIS, however, does not lead to any significant changes in atmospheric CO_2. The climate signature of a WAIS collapse is structurally consistent with available paleoproxy signals of the last interglacial MIS5e.

1. Introduction

[2] The West Antarctic Ice Sheet (WAIS) is a marine-based ice sheet and may hence be very susceptible to variations in sea level and ocean temperature [*Bindschadler*, 1998]. Increasing sea level may destabilize the main ice shelves in Antarctica which may subsequently accelerate the flow of inland glaciers into the ocean and hence lead to further sea level rise. Moreover, subsurface ocean warming can destabilize the WAIS from below, triggering an erosion of the grounding line and leading to further melting [*Rignot and Jacobs*, 2002; *Payne et al.*, 2004]. The magnitude of these processes is very difficult to assess, which severely hampers our skill to predict global sea level rise in the coming centuries [*Oppenheimer and Alley*, 2004]. A partial collapse of the WAIS would lead to a global sea level rise of about 3 to 6 m [*Oppenheimer*, 1998; *Bamber et al.*, 2009].

[3] Presence of young diatoms and relatively high levels of Beryllium in late Pleistocene sediments from the Ross Sea indicate that the WAIS retreated substantially during interglacial periods of the Pleistocene [*Scherer et al.*, 1998]. Recent paleostudies [*Hearty et al.*, 2007; *Carr et al.*, 2010]

showed that the sea level was up to 9 m higher than today during Marine Isotope Stage 5e (MIS5e, ~123 ka B.P.), making MIS5e an interesting candidate to study the potential collapse of the WAIS [*Mercer*, 1978]. In addition, a combined ice sheet/ice shelf model simulated several WAIS collapses during the Pleistocene [*Pollard and DeConto*, 2009] in phase with strong austral summer insolation anomalies. During MIS5e, the model simulated a significant retreat of the WAIS, but not a complete collapse.

[4] Variations in benthic $\delta^{18}O$ and abundance of diatoms in a marine sediment core from the Ross Sea indicated orbitally paced retreats of the WAIS during the Pliocene [*Naish et al.*, 2009]. This finding was also confirmed by the Antarctic ice sheet modeling study [*Pollard and DeConto*, 2009]. Considering that the WAIS retreated substantially in the past, when the Antarctic climate was about 3°C warmer than today [*Kim and Crowley*, 2000] and the atmospheric CO_2 was as high as 400 ppmv [*Van Der Burgh et al.*, 1993; *Raymo et al.*, 1996; *Pagani et al.*, 2010], the WAIS could potentially retreat as a result of increasing greenhouse gases in the future. It is therefore timely to better understand the possible consequences of a WAIS retreat onto the climate and the biogeochemical cycle.

[5] Recent modeling studies have documented the climate response to massive meltwater pulses into the Southern Ocean. Using state-of-the-art coupled general circulation models, *Richardson et al.* [2005], *Stouffer et al.* [2007] and *Ma et al.* [2010] find that the addition of freshwater at high southern latitudes leads to a stabilization of the water column,

---

[1]Climate and Environmental Physics, Oeschger Centre for Climate Change Research, University of Bern, Bern, Switzerland.
[2]IPRC, SOEST, University of Hawai'i, Honolulu, Hawaii, USA.
[3]Département AGO, Université de Liège, Liège, Belgium.

Table 1. Idealized Southern Ocean Freshwater Pulse Experiments[a]

	Maximum Freshwater Input	Freshwater Input Duration	Conditions	Climate Analog
WAIS$_{400}$	0.35 Sv	400 years	PI	Pleistocene IG
WAIS$_{800}$	0.18 Sv	800 years	PI	Pleistocene IG
WAIS$_{400-2CO2}$	0.35 Sv	400 years	2X CO_2	Pliocene - Future
WAIS$_{800-2CO2}$	0.18 Sv	800 years	2X CO_2	Pliocene - Future
CO2	none		2X CO_2	

[a]Shown are the maximum freshwater input, the total duration of the meltwater pulse, the climatic conditions under which the experiments were performed, and the climate analog. PI stands for preindustrial climate conditions, 2X CO_2 refers to atmospheric CO_2 doubling over 100 years then stabilization at 750 ppmv, Pleistocene IG stands for Pleistocene interglacial such as MIS5e. CO2 is a control CO_2 doubling experiment. LOCH is active in all experiments.

which inhibits deep convection and therefore the formation of Antarctic Bottom Water (AABW). At high southern latitudes, the surface air and ocean temperature decrease significantly, while an oceanic subsurface warming is simulated. Consistently, these modeling studies also demonstrate that Southern Hemispheric Westerlies strengthen in response to the freshwater perturbation. Moreover, due to a decrease of the meridional density gradient, the Antarctic Circumpolar Current (ACC) weakens in all of these modeling experiments.

[6] The biogeochemical response to Antarctic meltwater pulses has, to our knowledge, not been studied before. The main rationale of our study is to evaluate the impact of a rapid disintegration of the interglacial WAIS, on global climate and the carbon cycle using the Earth system model of intermediate complexity LOVECLIM. We expect that the derived climatic fingerprints of such an event could help in the interpretation of paleoclimate proxy data in the Southern Hemisphere.

[7] In section 2, we describe the experimental setup of our modeling experiments. Section 3 focuses on the climate and biogeochemical response to a collapse of the WAIS during interglacials of the Pleistocene and CO_2 doubling conditions. A previously overlooked positive feedback between ice sheet and ocean that might lead to an accelerated disintegration of the WAIS is also described. Finally, section 4 discusses our main results in the light of past and future climate change.

2. Experimental Setup

[8] The model used in this study is the model of intermediate complexity LOVECLIM (LOch-Vecode-Ecbilt-CLio-agIsm Model), version 1.1. The atmospheric component of the coupled model LOVECLIM is ECBilt [*Opsteegh et al.*, 1998], a spectral T21, three-level model, based on quasi-geostrophic equations extended by estimates of the neglected ageostrophic terms [*Lim et al.*, 1991] in order to close the equations at the equator. The sea ice-ocean component of LOVECLIM, CLIO [*Goosse et al.*, 1999; *Goosse and Fichefet*, 1999; *Campin and Goosse*, 1999] consists of a free-surface primitive equation model with 3° × 3° resolution, coupled to a thermodynamic-dynamic sea ice model. Coupling between atmosphere and ocean is done via the exchange of freshwater, momentum and heat fluxes.

[9] The terrestrial vegetation module of LOVECLIM, VECODE [*Brovkin et al.*, 1997] has recently been coupled to the LOVECLIM model [*Renssen et al.*, 2005]. VECODE simulates the dynamical vegetation changes and the terrestrial carbon cycle in response to climatic conditions (annual mean temperatures, annual precipitation and other derived climatic quantities such as growing degree days, seasonality of rainfall). Two plant functional types, grass and trees, describe the vegetation cover. For each land grid cell, VECODE calculates the fractional coverage with grass and trees and the fractional desert area. Terrestrial net primary production is a function of temperature and precipitation as well as atmospheric CO_2 concentrations. The produced organic carbon is aggregated in four compartments: leaves, stems and roots, woody residues, and dead organic matter in the soil (humus). The conversion rates among these four terrestrial carbon reservoirs have characteristic time scales ranging from 1 year to 800 years. The conversion rates depend on primary production and temperature. A more detailed description is given in *Brovkin et al.* [2002]. In the LOVECLIM version employed here, the feedback from the vegetation to the atmosphere is only given by surface albedo changes. Other factors such as evapotranspiration and surface roughness are neglected.

[10] LOCH is a three-dimensional global model of the oceanic carbon cycle *Mouchet and Francois* [1996]. The present version of the model is described by *Goosse et al.* [2010]. The prognostic state variables considered in the model are dissolved inorganic carbon (DIC), total alkalinity, phosphates (PO_4^{3-}), organic products, oxygen and silica. LOCH is fully coupled to CLIO, with the same time step. In addition to their biogeochemical transformations tracers in LOCH experience the circulation field predicted by CLIO. LOCH computes the export production from the fate of a phytoplankton pool in the euphotic zone (0–120 m). The phytoplankton growth depends on the availability of nutrients (PO_4^{3-}) and light, with a weak temperature dependence. A grazing process together with natural mortality limit the primary producers biomass and provide the source term for the organic matter sinking to depth. The other processes described in the model include remineralization, carbonate precipitation and dissolution as well as opal production. LOCH does not include sedimentary processes but nevertheless takes into account carbonate compensation mechanisms. The atmospheric CO_2 content is updated for each ocean time step.
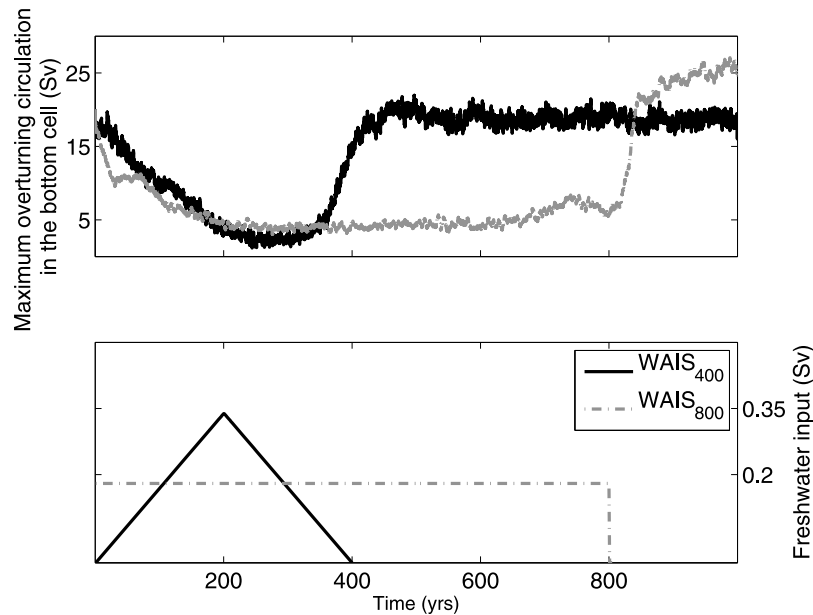
Figure 1. (top) Maximum overturning circulation in the bottom cell of the Southern Ocean (Sv) for experiments $WAIS_{400}$ (black) and $WAIS_{800}$ (dashed grey). (bottom) Anomalous freshwater flux in the Southern Ocean (Sv) for experiments $WAIS_{400}$ (black) and $WAIS_{800}$ (dashed grey).

[11] To estimate the impact of a collapse of the West Antarctic Ice Sheet during interglacial periods on the climate and carbon cycle, we perform a set of highly idealized experiments (Table 1). To mimic a rapid disintegration of the WAIS, we assume an idealized freshwater release of about 2.2×10^6 km^3 into the area 163°E–11°E, 70°S–80°S, which encompasses the Ross, Amundsen, Bellingshausen and Weddell Seas. This scenario is reasonable given the estimates of *Lythe et al.* [2001]: the total volume of the present-day WAIS including ice shelves and the volume of the grounded ice sheet below sea level are 3.6×10^6 km^3 and 1×10^6 km^3, respectively. As *Oppenheimer* [1998] estimated the mean time to collapse the WAIS in the future at 500 to 700 years, we designed two scenarios in which a collapse is obtained in 400 and 800 years, respectively.

[12] In experiment $WAIS_{400}$, we prescribe a triangular-shaped freshwater pulse with a total duration of 400 years attaining a maximum strength of 0.35 Sv after 200 years (Figure 1, bottom left). Once the freshwater input ceases we let the model run for another 600 years. In experiment $WAIS_{800}$, the freshwater input is set constant at 0.18 Sv and has a total duration of 800 years. Experiments $WAIS_{400}$ and $WAIS_{800}$ are performed under preindustrial conditions, start from experiment PIN and serve as analogs of interglacial times of the Pleistocene such as MIS5e. The pre-industrial steady state (PIN) was obtained by forcing LOVECLIM with 278 ppmv of atmospheric CO_2 during 500 years, then allowing the atmospheric CO_2 to vary freely during 2000 years.

[13] *Naish et al.* [2009] and *Pollard and DeConto* [2009] also suggested that collapses of the WAIS occurred during the Pliocene when the climate was about 3°C warmer than today [*Kim and Crowley*, 2000] and the atmospheric CO_2 was as high as 400 ppmv [*Van Der Burgh et al.*, 1993;

Raymo et al., 1996; *Pagani et al.*, 2010]. Since in the version of LOVECLIM used here, an atmospheric CO_2 doubling leads to a $\sim$ 3°C increase in global mean temperature, we perform two additional experiments, called $WAIS_{400-2CO_2}$ and $WAIS_{800-2CO_2}$, forced with an atmospheric CO_2 content of 750 ppmv. From these experiments we can then evaluate the impact of a collapse of the WAIS for future climate and Pliocene conditions.

[14] Experiments $WAIS_{400-2CO_2}$ and $WAIS_{800-2CO_2}$ use the same freshwater forcing as $WAIS_{400}$ and $WAIS_{800}$. These experiments start from a present day run and are then transiently forced with linearly increasing CO_2 concentration attaining 750 ppmv in 100 years. The atmospheric CO_2 concentration is subsequently kept constant at 750 ppmv. Experiments $WAIS_{400-2CO_2}$ and $WAIS_{800-2CO_2}$ are compared to a control CO_2 doubling experiment ($C\overline{O}2$). CO2 is forced with the same atmospheric CO_2 forcing as in $WAIS_{400-2CO_2}$ but no freshwater pulse is applied.

[15] The experiments performed in this study are highly idealized, but given the uncertainty in our knowledge of the timing of past WAIS collapses, we think these idealized experiments provide a good first-order approximation of the climate and biogeochemical responses during interglacial WAIS retreats.

3. Impact of a WAIS Collapse During Interglacials and CO_2 Doubling Conditions

3.1. Climate Response

[16] The Southern Ocean freshwater perturbation prescribed in $WAIS_{400}$ leads to a freshening of the surface waters lowering the surface density (not shown) and increasing the stratification. The formation of a strong halocline and the associated increased stability of the water
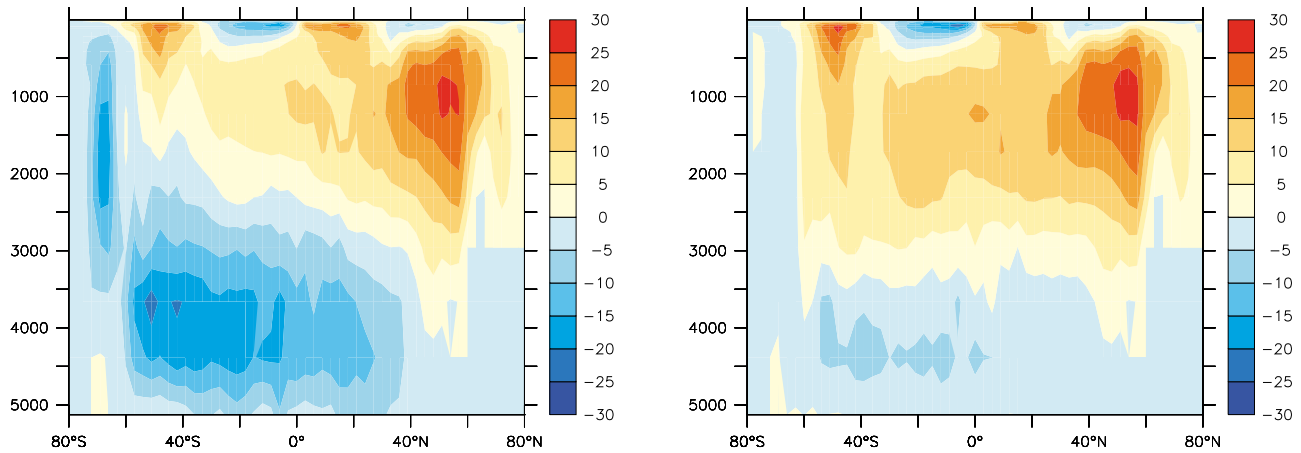
Figure 2. Stream function (Sv) averaged globally for (left) PIN and (right) over years 200–250 for experiment WAIS$_{400}$.

column inhibit deep convection in the Southern Ocean (not shown) thus leading to a breakdown of Antarctic Bottom Water (AABW) formation. This is evidenced in the globally averaged meridional stream function (Figure 2). The bottom overturning cell that is associated with the formation of AABW reduces in strength from 17 to 3 Sv (Figure 1). These large-scale transport changes of AABW in turn increase the cross-equatorial export of North Atlantic Deep Water (NADW) into the Southern Hemisphere. Relatively warm NADW has to upwell in the Southern Ocean, which has a secondary effect on the stratification field in the Southern Ocean.

[17] As waters are relatively warm at depth in the Southern Ocean, the reduced deep convection leads to a cooling of the ocean's surface [*Zhang*, 2007]. In the latitudinal band 60°S–20°S, the surface waters cool by up to 4°C in experiment WAIS$_{400}$ (Figure 3, left). South of 60°S, the

temperature of the surface water is basically unchanged as its annual mean temperature is already close to the freezing point. Moreover, the greater near-surface stratification induces a shoaling of the annual mixed layer in the latitudinal band 80°S–52°S by 50–150 m. Cold winds in austral fall and winter can then cool the shallower mixed layer more efficiently, which also contributes to surface cooling and enhanced formation of sea ice.

[18] Due to the anomalously fresh surface water near Antarctica, the surface density is significantly reduced, which leads to a poleward shift of the outcropping isopycnals south of 40°S and a reduced slope of the isopycnals (not shown). In LOVECLIM, the eddy-induced mixing is parameterized using the Gent-McWilliams scheme [*Gent et al.*, 1995]. Isopycnals slopes flatten considerably, leading to a near collapse of the bolus velocity in the depth range 20–200 m. This induces a weakening of the meridional heat
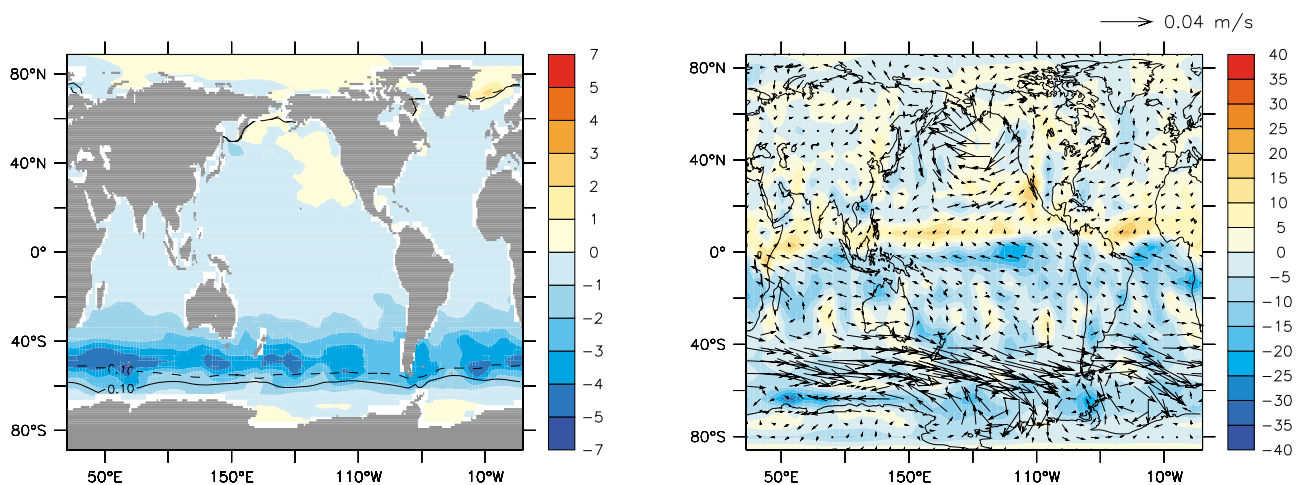

Figure 3. (left) Sea surface temperature anomalies (°C) averaged over years 200–250 for experiment WAIS$_{400}$. Contours represent the 0.1 m annual sea ice margin for PIN (solid line) and years 200–250 for experiment WAIS$_{400}$ (dashed line). (right) Precipitation anomalies (cm/yr) and wind stress anomalies averaged over years 200–250 for WAIS$_{400}$.

transport to high southern latitudes [*Stocker et al.*, 2007]. The estimated bolus heat flux anomaly (see *Stocker et al.* [2007] for details of the calculation) amounts to about −0.11 K/year at year 200 over the latitudinal band 55°S–65° S and in the depth range 20–250 m. This is equivalent to a decrease in heat transport of about 0.08 PW, which may explain a fraction of the 0.7°C cooling seen in this area.

[19] These surface cooling processes are further amplified by the sea ice albedo feedback. The annual mean sea ice margin shifts equatorward by 4° during the Southern Ocean freshwater pulse phase, reaching the Southern tip of South America (Figure 3). Increased surface albedo due to the simulated sea ice expansion cools the lower atmosphere by about 4°C.

[20] Under CO_2 doubling conditions, the results are qualitatively similar to those under preindustrial conditions; however, the amplitude of the changes is greater in $WAIS_{800}$ $_{-2CO2}$ than in $WAIS_{800}$. In experiment $WAIS_{400-2CO2}$ the ocean surface also cools by up to 4°C in the latitudinal band 40°S–60°S compared to CO2 and the sea ice retreats more slowly in the Southern Ocean. Moreover, at year 200, the annual sea ice edge extends about 5° equatorward in the Pacific and Atlantic sectors of the Southern Ocean for $WAIS_{400-2CO2}$ compared to CO2. As a result the lower atmosphere over the latitudinal band 60°S–90°S is about 4°C cooler in $WAIS_{400-2CO2}$ compared to CO2.

[21] Two mechanisms have recently been proposed to explain the cooling response of the Southern Hemisphere north of Drake passage: wave propagation [*Ivchenko et al.*, 2006] and the Wind-Evaporation SST (WES) feedback [*Ma et al.*, 2010]. We found that the WES feedback plays an important role in cooling the Southern Hemisphere equatorward of the Subtropical Front. The WES feedback results from the fact that negative SST anomalies in the eastern parts of the southern ocean basins are accompanied by strengthened trade winds, which lead to enhanced cooling via increased evaporation.

[22] In response to the freshwater forcing and the resulting SST and sea ice anomalies, Southern Hemispheric Westerlies intensify substantially (Figure 3, right). The meridional temperature gradient increase between 20°S and 50°S is responsible for the wind intensification through the thermal wind balance. By enhancing evaporation of the surface waters, the stronger Westerlies contribute to the cooling of surface waters in the latitudinal band 50°S–35°S. In addition, the enhanced Westerlies lead to stronger upwelling at about 60°S and increased northward Ekman transport.

[23] In spite of an intensification of the zonally averaged Southern Hemispheric Westerlies by about 20%, the Antarctic Circumpolar Current (ACC) weakens by about 25%. This can be explained by a reduction of the meridional density gradient induced by low saline surface waters near Antarctica and the associated geostrophic response of the ACC.

[24] In the Northern Hemisphere, a significant warming response is found over a small area in the northern North Atlantic (50°W–0°, 60°N–80°N) (Figure 3, left). Such a feature was also simulated by *Richardson et al.* [2005], *Stouffer et al.* [2007] and *Ma et al.* [2010], even though the specific location where this warming occurred appears to be

strongly model dependent. The warming simulated by *Richardson et al.* [2005] is located in the Labrador and Irminger Seas, while *Ma et al.* [2010] obtain a warming at about 50°N over the Pacific and Atlantic Oceans. *Stouffer et al.* [2007] do not describe the regional details of the warming obtained at high northern latitude.

[25] The enhanced temperature gradient in the Southern Hemisphere induces a strengthening of the southeasterly trade winds, while the reduced temperature gradient in the Northern Hemisphere leads to a weakening of the northeasterly trades (Figure 3, right). The inter hemispheric SST gradient induces a northward shift of the ITCZ and thus drier conditions in the Southern Hemisphere and wetter conditions in the Northern Hemisphere.

[26] The climatic changes discussed above are observed during the four seasons but are slightly more pronounced during austral winter.

[27] The climate response to a Southern Ocean meltwater pulse obtained with LOVECLIM is quite similar to the one obtained with more complex models such as HadCM3 [*Richardson et al.*, 2005], FOAM [*Ma et al.*, 2010] and the GFDL R30 model [*Stouffer et al.*, 2007]. A more detailed description of the climate response to Southern Ocean meltwater pulses obtained with the LOVECLIM Earth system model is also provided by *Swingedouw et al.* [2009].

[28] As already discussed by *Swingedouw et al.* [2009], the duration and amplitude of the Southern Hemispheric meltwater pulse play an important role in determining the overall characteristics of the climate response. As can be seen in Figure 4, the duration of the climatic response is a function of the length of the meltwater pulse. After resuming to unperturbed conditions, the Southern Ocean salinity anomaly (Figure 4, top left) dissipates quickly due to the northward Ekman transport and the upwelling of Circumpolar Deep Waters (CDW), in accordance with the results of *Trevena et al.* [2008]. Less than 10 years after the end of the meltwater pulse the Southern Ocean salinity anomaly has dissipated for all experiments, irrespective of the background climate conditions.

[29] We also find that the amplitudes of the Southern Ocean climate anomalies are proportional to the rate of meltwater discharge. Air temperature anomalies averaged over 60°S–90°S amount to about −4.2°C for $WAIS_{400}$ and −1°C for $WAIS_{800}$ (Figure 4, top right).

3.2. Subsurface Warming in the Southern Ocean

[30] Changes in stratification, mixing, convection and Ekman pumping in the Southern Ocean also lead to substantial subsurface temperature anomalies (Figure 5). Subsurface temperatures at depths of 500–1500 m and south of 60°S increase by up to 1.1°C in $WAIS_{400}$. This warming can be attributed to the fact that deep convection near Antarctica and the formation of AABW are strongly inhibited due to the freshwater perturbation. A similar subsurface warming was obtained as a result of the suppression of the AABW formation due to weaker Southern Hemispheric Westerlies [*Menviel et al.*, 2008]. In the Ross and Weddell Seas cold AABW is replaced by warmer Circumpolar Deep Waters (CDW). A temperature-salinity scatterplot of the Southern Ocean waters (not shown) indicates that during the period of
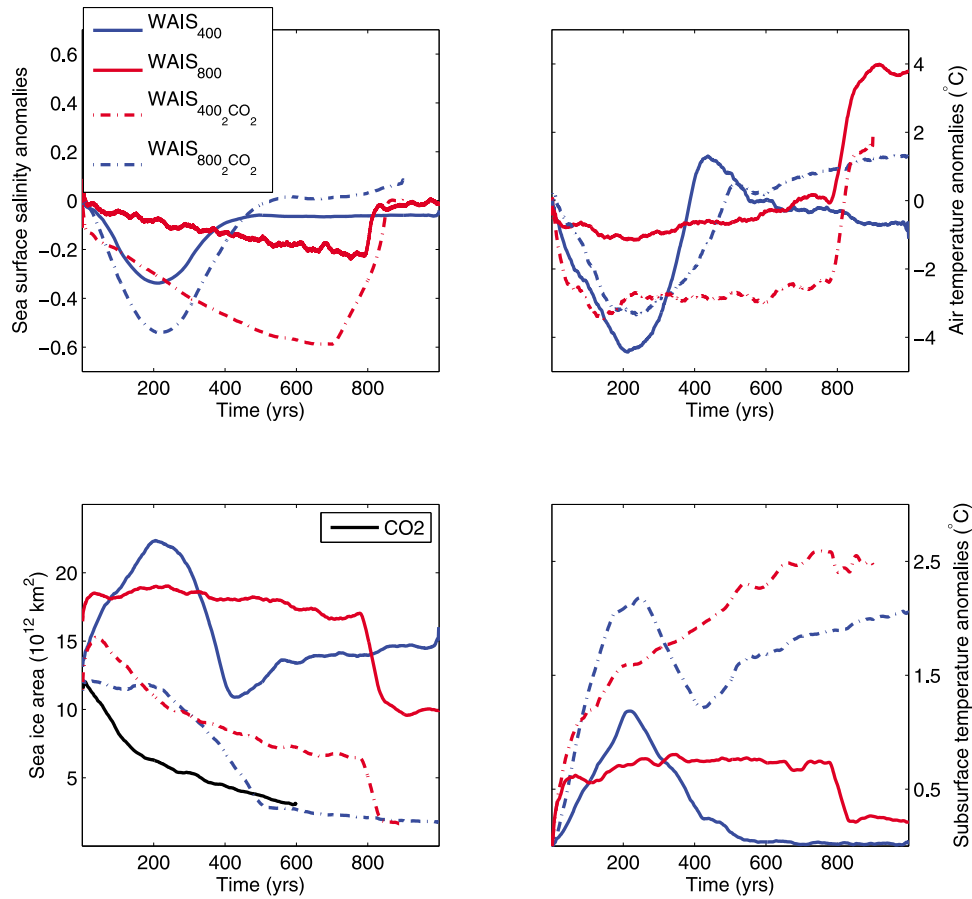
Figure 4. Time series of (top left) sea surface salinity anomalies averaged over 60°S–90°S (psu), (top right) 2 m air temperature anomalies averaged over 60°S–90°S (°C), (bottom left) Southern Hemisphere annual sea ice area ($\times 10^{12}$ m^2), and (bottom right) subsurface temperature anomalies averaged over 160° E–300°E, 60°S–80°S, 500–1000 m for experiments WAIS$_{400}$ (solid blue line), WAIS$_{800}$ (solid red line), WAIS$_{400-2CO2}$ (dashed blue line), and WAIS$_{800-2CO2}$ (dashed red line). The air and subsurface temperature anomalies for experiments WAIS$_{400-2CO2}$ and WAIS$_{800-2CO2}$ are calculated against the control experimentCO2. Figure 4 (bottom left) also shows the Southern Hemisphere sea ice area for CO2 (black line).
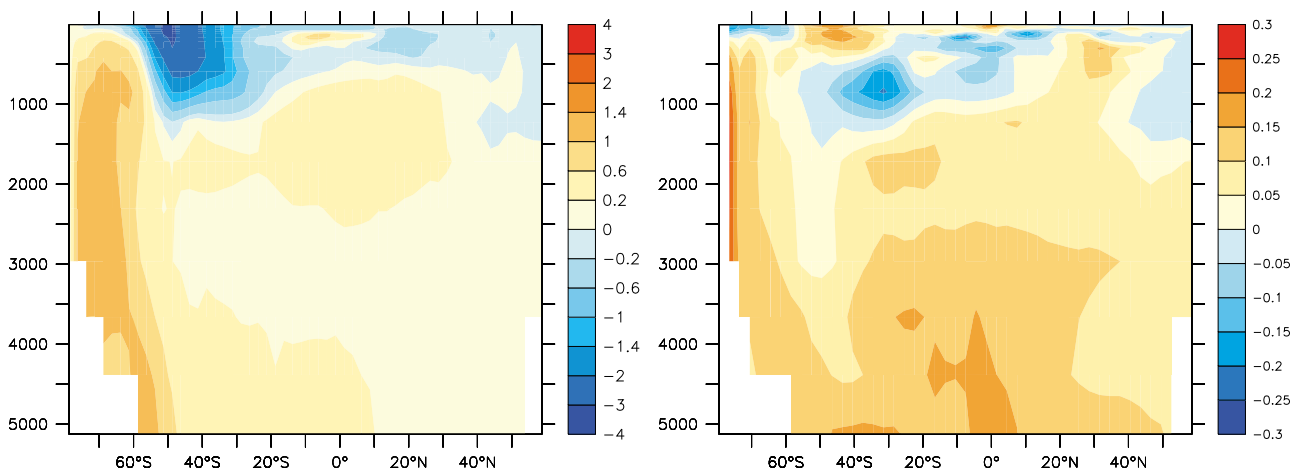
Figure 5. (left) Ocean temperature anomalies (°C) and (right) phosphate content anomalies (μmol/L) averaged over the Pacific basin and over years 200–250 for experiment WAIS$_{400}$.
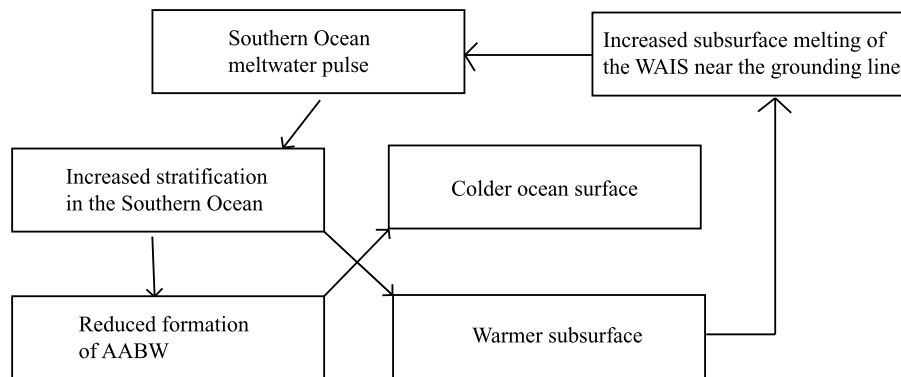
Figure 6. Schematic representation of the positive feedback involved in subsurface temperature increase and ice sheet melting.

reduced Bottom Water formation, Circumpolar Deep water (CDW) fills most of the intermediate and deep Southern Ocean.

[31] Figure 4 (bottom right) shows the ocean temperature anomalies averaged over 60°S–80°S, 160°E–60°W and over 500–1000 m depth. The anomalies generated amount to about 1.2°C for WAIS$_{400}$ and 0.7°C for WAIS$_{800}$, respectively. Under CO_2 doubling conditions, the subsurface temperature increase in the Southern Ocean is even more pronounced. The anomalies compared to CO2 amount to 2.2°C for WAIS$_{400-2CO2}$ and 2.5°C for WAIS$_{800-2CO2}$.

[32] Other coupled modeling studies also simulated a subsurface water warming near Antarctica of about 1.5°C [*Stouffer et al.*, 2007; *Trevena et al.*, 2008; *Ma et al.*, 2010; *Swingedouw et al.*, 2009] due to reduced formation of cold AABW. *Trevena et al.*'s [2008] modeling study is performed with an OGCM coupled to an Energy Balance Model (EBM) that uses fixed climatological winds. A significant subsurface warming was simulated, without the intensification of the Southern Hemispheric Westerlies found in more complex models. Moreover, using LOVE-CLIM, *Swingedouw et al.* [2009] conducted a Southern Ocean meltwater experiment with fixed climatological pre-industrial winds. In this experiment a ~ 2°C subsurface warming was simulated at high southern latitudes, suggesting that changes in the surface winds do not play a major role in the high southern latitude subsurface warming during the Southern Ocean freshwater pulse experiment.

[33] The West Antarctic Ice Sheet grounding line in the Ross Sea reaches on average a depth of about 500 m below sea level, whereas the Ross Sea has an average depth of about 1000 m. Here we hypothesize that warmer subsurface waters underneath the Ross Sea shelf that are caused by a reduction of AABW and an intrusion of CDW may erode the grounding line of the WAIS, thereby accelerating the melting of the WAIS, increasing the freshwater flux into the Southern Ocean and thus providing a positive feedback for the ice sheet retreat, as illustrated in Figure 6.

[34] Observations as well as modeling studies indicate that a subsurface warming similar to the one obtained in WAIS$_{800}$ would lead to a significant increase in basal ice shelf melting [*Rignot and Jacobs*, 2002; *Hattermann and*

Levermann, 2010] and could eventually provide a significant positive feedback on the melting of the WAIS.

[35] A more accurate estimate of the magnitude of this positive ocean-ice sheet feedback would, however, require more detailed modeling studies using high-resolution coupled ocean-ice shelf and ice sheet models. It should also be noted that coarse-resolution models such as LOVECLIM do not fully resolve the details of the processes that lead to Antarctic Bottom Water formation and the potential intrusion of CDW into the convection regions in the Ross and Weddell Seas during phases of weak AABW formation.

3.3. Carbon Cycle Response

[36] Due to the stronger Southern Hemispheric Westerlies, upwelling in large areas of the Southern Ocean is enhanced in experiment WAIS$_{400}$ (contours in Figure 7, top). As a result, the nutrient supply to the euphotic zone increases (Figure 7, top). Although euphotic zone phosphate and silicate content increase by 20% and 40%, respectively, in the latitudinal band 30°S–50°S, export production and nutrient utilization efficiency decrease by 25% and 30%, respectively, in the latitudinal band 40°S–60°S (Figure 7, bottom). Export production is thus not limited by nutrient availability, but rather by the reduced availability of light in response to the sea ice advance. On the other hand, due to the stronger wind, more nutrients are advected by the South Antarctic Mode Water (SAMW) to the mid and low latitudes. This is documented by a greater phosphate content in the latitudinal band 20°–60°S and above 500 m depth (Figure 5, right). This increased northward advection of nutrient-rich waters into the mid and low latitudes of the Southern Hemisphere leads to a 15% increase in averaged export production in the latitudinal band 0°–40°S. In the northern North Atlantic, the export production increases slightly due to sea ice retreat and warmer conditions. In spite of these large regional differences, there is no substantial change in globally averaged export production.

[37] Similar changes in export production are observed in experiments WAIS$_{800}$, WAIS$_{400-2CO2}$ and WAIS$_{800-2CO2}$.

[38] The oceanic sink of CO_2 south of 40°S increases slightly in experiment WAIS$_{400}$ due to increased solubility caused by the surface cooling and stronger winds. Any-
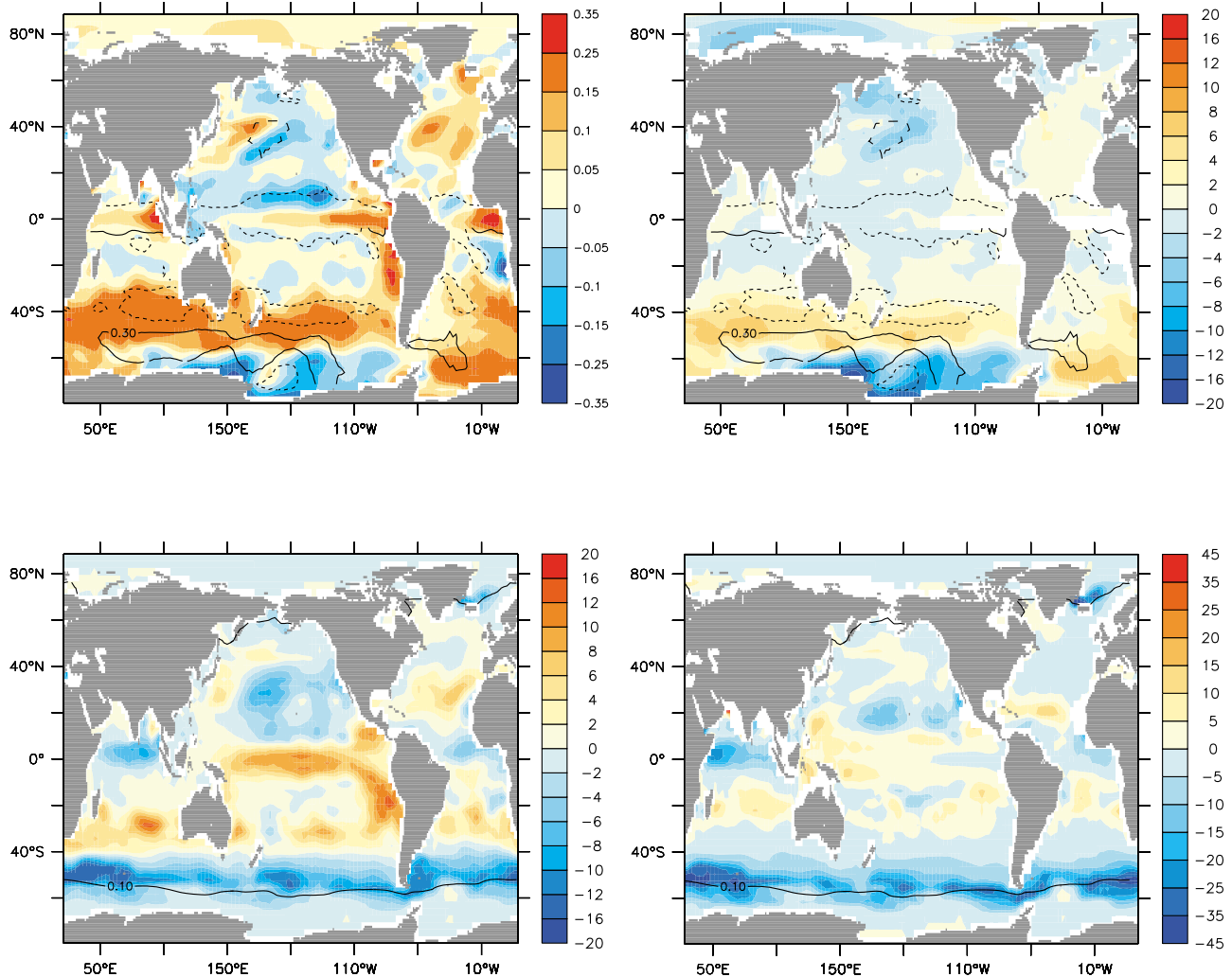
Figure 7. (top left) Phosphate content (μmol/L) anomalies averaged over the euphotic zone and over years 200–250 for WAIS$_{400}$ compared to PIN. (top right) Silicate content (μmol/L) anomalies averaged over the euphotic zone and over years 200–250 for WAIS$_{400}$ compared to PIN. The contours represent Ekman pumping anomalies at (+) or (−) 0.3×10^{-6} m/s. A positive Ekman pumping represents an upwelling area. To prevent discontinuities, the Ekman pumping values in the latitudinal band 5°S–5°N were omitted. (bottom left) Export production anomalies (gC/m^2/yr) for years 200–250 of experiment WAIS$_{400}$ compared to PIN. (bottom right) Nutrient utilization efficiency anomalies for years 200–250 of experiment WAIS$_{400}$ compared to PIN. Nutrient utilization efficiency is calculated as $(1 - [PO_4]_{surf}/[PO_4]_{deep}) \times 100$, where $[PO_4]_{surf}$ and $[PO_4]_{deep}$ are the phosphate content in the euphotic zone and in the deep ocean, respectively. The contour represents the annual mean sea ice extent (0.1 m) for years 200–250 of experiment WAIS$_{400}$.

where else the changes in air-sea CO_2 flux are insignificant. The ocean is thus acting as a weak sink of CO_2, and the marine carbon storage increases by about 20 Gt for experiment WAIS$_{400}$.

[39] Due to the drier and colder conditions prevailing in the Southern Hemisphere, the terrestrial primary production decreases and therefore the carbon storage on land is reduced. The carbon stored in the latitudinal band 10°S–30°S decreases by about 5% during the first 200 years of WAIS$_{400}$. On the other hand, the wetter conditions prevailing in the northern tropics lead to a small increase of carbon storage in the latitudinal band 0°–20°N (+5%). The terrestrial carbon storage significantly increases in the Sahara region as a result of increased precipitation. Averaged globally, the terrestrial carbon stock decreases by about 25 GtC. In experiment WAIS$_{400}$, the atmospheric CO_2 content increases by only 2.5 ppmv (not shown).

[40] Irrespective of the background conditions and the magnitude or length of the freshwater addition in the Southern Ocean, the AABW weakening does not lead to
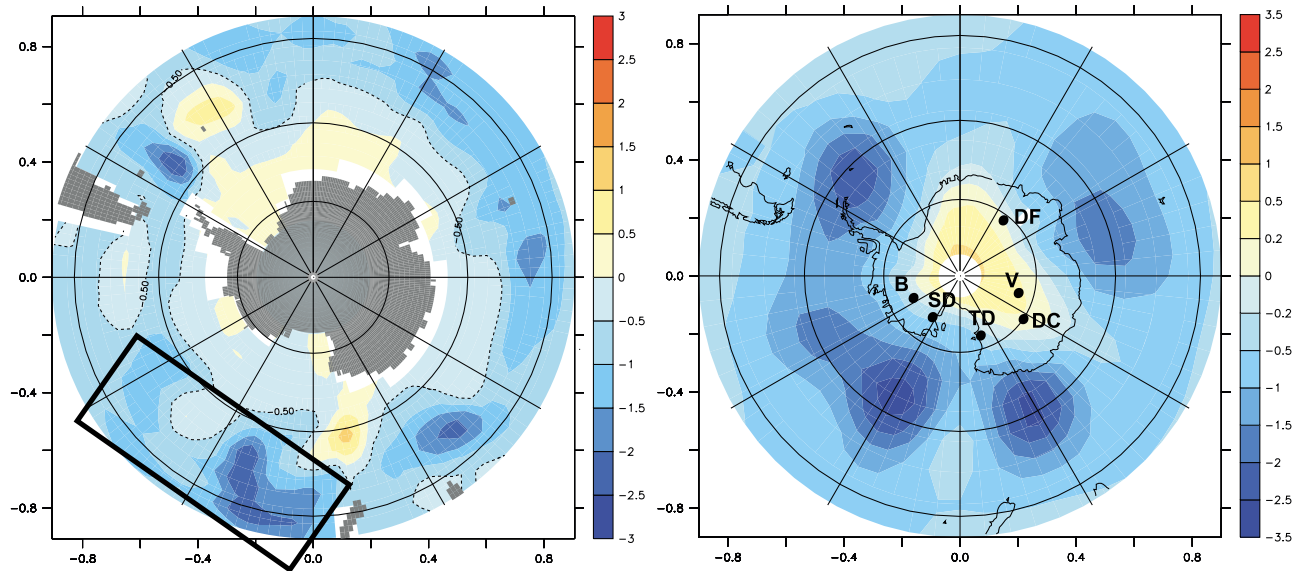
Figure 8. (left) Annual SST anomalies over the Southern Ocean averaged over years 500–600 of experiment WAIS$_{800}$ and compared to PIN. The rectangle shows the area where a cooling due to a WAIS collapse is most likely to be recorded. (right) SON 2 m air temperature anomalies over Antarctica averaged over years 500–600 of experiment WAIS$_{800}$ and compared to PIN. DF stands for Dome Fuji, V is for Vostok station, DC is for EPICA Dome C, TD is for Taylor Dome, SD is for Siple Dome, and B is for Byrd station.

significant changes in the size of the different carbon reservoirs.

4. Discussion and Conclusion

[41] Our model results show that a Southern Ocean meltwater pulse leads to a significant cooling over Antarctica as well as in the Southern Ocean. Even though the Southern Hemisphere Westerlies strengthen significantly, the ACC weakens. These results are in overall qualitative agreement with other Southern Ocean meltwater pulse studies performed with CGCMs [*Richardson et al.*, 2005; *Stouffer et al.*, 2007; *Ma et al.*, 2010] under interglacial conditions. We found that an increase of sea ice leads to a decrease in marine export production south of 40°S. However, it should be noted that our model does not include iron limitation. Changes in export production therefore do not take into account any possible changes in iron supply to the euphotic zone, nor do they capture different non-Redfield processes. In contrast, the greater transport of nutrients from high southern latitudes to low latitude leads to enhanced marine export production in the latitudinal band 0°–40°S. Overall, the addition of freshwater in the Southern Ocean does not lead to significant changes in the different carbon reservoirs.

[42] In our simulations a rapid collapse of the WAIS leads to a weakening of the AABW formation. A potential fingerprint of a WAIS meltwater pulse in paleorecords is a negative excursion in benthic δ^{13}C records from the deep South Atlantic and Pacific. Moreover, as documented in Figure 8, we also expect a concomitant cooling of the Southern Ocean in the latitudinal band 40°–60°S. The area

southeast of New Zealand in our simulations is a good location to identify the climatic impact of a WAIS collapse. Over Antarctica the cooling is maximum along the coast and vanishes toward the interior. Ice core records from the Taylor Dome area would record a cooling that would not necessarily be seen at EPICA Dome C, Dome Fuji or Vostok station. During massive retreats of the WAIS and intrusions of sea water into large areas of Mary Byrd Land, the area around Siple Dome could become submerged, while ice flow could accelerate in the region around Byrd station. Usable data from Byrd and Siple Dome ice cores thus have to postdate the last significant retreat of the WAIS. Byrd and Siple Dome ice cores were drilled close to bed rock. The oldest age of ice reconstructed in Siple Dome is 97 ka B.P., 30 cm away from the bedrock (E. Saltzman, personal communication, 2010). Ice core data thus do not contradict the fact that a significant retreat of the WAIS could have occurred during MIS5e.

[43] Austral summer insolation at 70°S was very high at 118 ka B.P. and, as can be seen in Figure 9 (top), the *Pollard and DeConto* [2009] model simulation predicts a strong retreat of the WAIS at that time leading to a meltwater pulse in the Southern Ocean. Between 126 and 123 ka B.P., a negative excursion is seen in the benthic δ^{13}C record from marine sediment cores MD97-2120 [*Pahnke and Zahn*, 2005], ODP 1089 [*Hodell et al.*, 2003], RC11-83 and TN057-6 [*Ninnemann and Charles*, 2002] (Figure 9, bottom) that coincides with the model-diagnosed meltwater flux into the Southern Ocean. During the same time period, global sea level was about 9 m higher than at present [*Hearty et al.*, 2007; *Carr et al.*, 2010], which might be
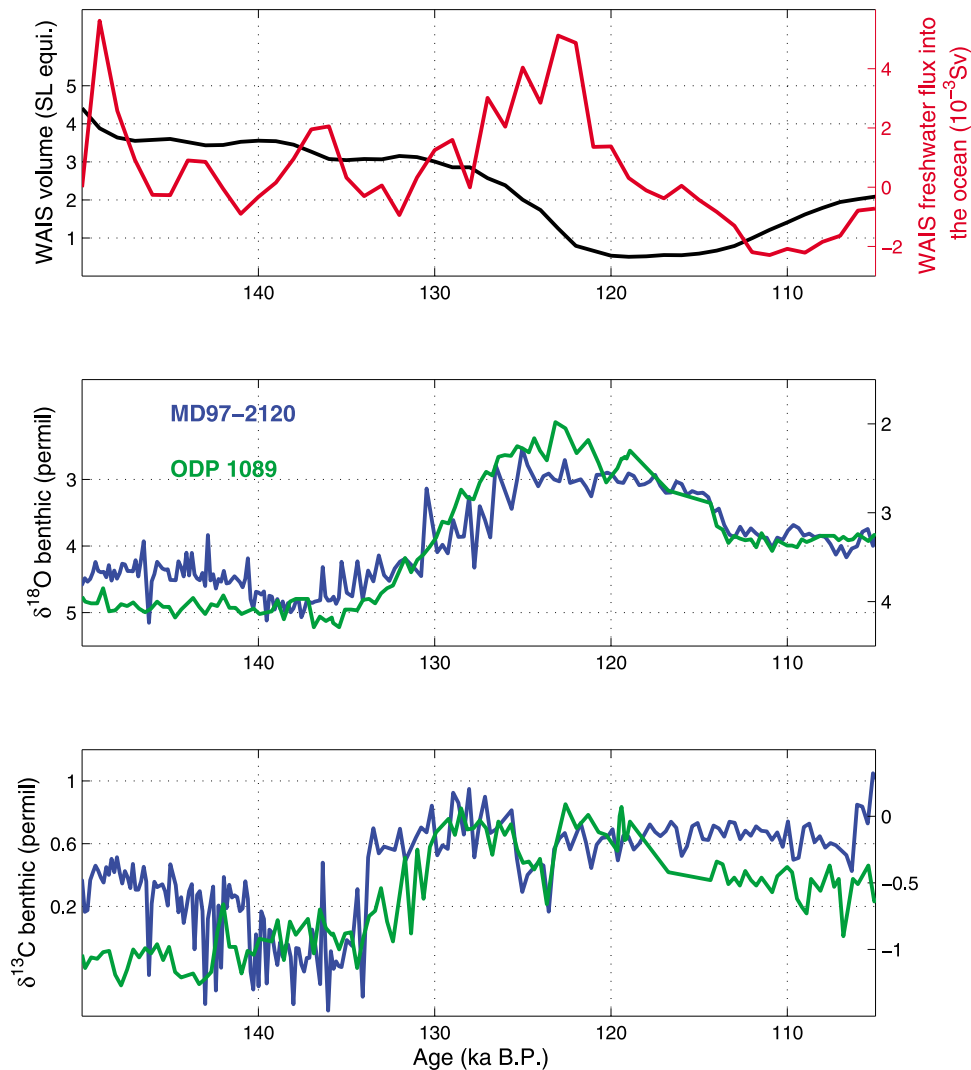
Figure 9. (top) Simulated WAIS ice volume in sea level equivalent [*Pollard and DeConto*, 2009] (black, m) and diagnosed WAIS meltwater flux into the Southern Ocean from *Pollard and DeConto* [2009] simulation (red, 10^{-3} Sv). (middle) Benthic δ^{18}O (permil) from marine sediment cores MD97-2120 (blue, left axis) [*Pahnke and Zahn*, 2005] and ODP 1089 (green, right axis) [*Hodell et al.*, 2003]. (bottom) Benthic δ^{13}C (permil) from marine sediment cores MD97-2120 (blue, left axis) [*Pahnke and Zahn*, 2005] and ODP 1089 (green, right axis) [*Hodell et al.*, 2003].

explained in part by a retreat of the WAIS [*Pollard and DeConto*, 2009].

[44] Southern Ocean paleoproxies are not inconsistent with the notion that a collapse of the WAIS could have occurred during MIS5e but higher-resolution paleorecords as well as modeling studies of MIS5e are needed to confirm this hypothesis. *Pahnke and Zahn* [2005] noted the recurrent nature of the negative benthic δ^{13}C at the end of glacial terminations I through IV in marine sediment cores MD97-2120 and ODP 1089. In addition these negative δ^{13}C shifts were associated with a cooling at high southern latitudes, making them good candidates for significant retreats of the WAIS. While *Pollard and DeConto* [2009] also simulated recurring collapses of the WAIS, the timing is slightly different from the negative benthic δ^{13}C anomalies seen in

marine sediment cores MD97-2120 and ODP 1089. Highly resolved paleodata from the high southern latitudes covering MIS7, MIS9, MIS11 or other previous interglacial periods of the Pleistocene could shed further light onto the stability of WAIS during interglacials. Numerical simulations of the WAIS extent, similar to the one performed by *Pollard and DeConto* [2009] but with a more comprehensive forcing parametrization could help to further constrain the timing of the WAIS collapse.

[45] A cooling of the Southern Ocean [*Pahnke and Zahn*, 2005; *Barker et al.*, 2009] and Antarctic continent [*Jouzel et al.*, 2007] was also observed during the Antarctic Cold Reversal, which occurred during the last deglaciation (~14.5–12 ka B.P.). This break in the deglaciation trend could have been caused by partial melting of the glacial

WAIS into the Southern Ocean [*Weaver et al.*, 2003] as the glacial WAIS was significantly larger than at present [*Conway et al.*, 1999]. Transient modeling studies of the last deglaciation could shed light onto the possible role of southern origin freshwater pulses in shaping the Antarctic Cold Reversal. Additional paleorecords from the Southern Ocean would also provide further insight into the occurrence of meltwater pulses from the Antarctic ice sheet and their associated climate and biogeochemical responses.

[46] As a collapse of the WAIS probably occurred in the past, further warming in the future due to increased greenhouse gas content in the atmosphere could also induce a significant retreat of the WAIS. Under CO_2 doubling conditions and according to our model simulations the rapid addition of freshwater into the Southern Ocean leads to a negative feedback in the lower atmosphere and at the surface of the ocean. The lower atmosphere air temperature and the temperature at the surface of the Southern Ocean increase more slowly when the AABW is weakened. The retreat of the Southern Hemispheric sea ice edge is delayed in experiments $WAIS_{400-2CO2}$ and $WAIS_{800-2CO2}$ compared to experiment CO2. This negative feedback was already discussed by *Swingedouw et al.* [2008]. However, we have also shown that as a result of freshwater addition in the Southern Ocean, the subsurface temperature around the Antarctic coast increases significantly. Under present-day conditions, subsurface warming has been shown to accelerate the melting of Antarctic ice shelves and ice sheets at their grounding lines [*Rignot and Jacobs*, 2002; *Payne et al.*, 2004]. Several factors contribute to the large subsurface warming in the Southern Ocean: increased stratification, reduction of AABW formation as well as intrusion of CDW. This increase is even more pronounced under CO_2 doubling conditions than under preindustrial conditions, and could subsequently induce further melting of the Antarctic ice shelf and erode the WAIS near the ice sheet-ocean interface. A retreat of the WAIS in the future could thus be accelerated through this positive feedback.

[47] In this study, to simulate a collapse of the WAIS, freshwater was added over an area extending from the Ross to the Weddell Sea. In reality, when the WAIS collapses, probably a massive iceberg release takes place, and only a part is directly released as liquid water. In a recent study, *Jongma et al.* [2009] suggested that a dynamic distribution of melting icebergs in the Southern Ocean might lead to less stratification compared to an homogeneous input of freshwater and therefore to a less efficient weakening of the AABW. In addition, the latent heat flux due to the melting iceberg might lead to enhanced formation of sea ice and greater brine rejection, providing a negative feedback to the AABW weakening. To better quantify the impact of a collapse of the WAIS on climate, a similar study should be performed with an interactive iceberg model.

References

Bamber, J. L., R. E. M. Riva, B. L. A. Vermeersen, and A. M. LeBrocq (2009), Reassessment of the potential sea-level rise from a collapse of the West Antarctic Ice Sheet, *Science*, *324*, 901–903, doi:10.1126/science.1169335.

Barker, S., P. Diz, M. J. Vautravers, J. Pike, G. Knorr, I. R. Hall, and W. S. Broecker (2009), Interhemispheric Atlantic seesaw response during the last deglaciation, *Nature*, *457*, 1097–1102, doi:10.1038/nature07770.

Bindschadler, R. A. (1998), The future of the West Antarctic Ice Sheet, *Science*, *282*, 428–429, doi:10.1126/science.282.5388.428.

Brovkin, V., A. Ganopolski, and Y. Svirezhev (1997), A continuous climate-vegetation classification for use in climate-biosphere studies, *Ecol. Modell.*, *101*, 251–261, doi:10.1016/S0304-3800(97)00049-5.

Brovkin, V., J. Bendtsen, M. Claussen, A. Ganopolski, C. Kubatzki, V. Petoukhov, and A. Andreev (2002), Carbon cycle, vegetation, and climate dynamics in the Holocene: Experiments with the CLIMBER-2 model, *Global Biogeochem. Cycles*, *16*(4), 1139, doi:10.1029/2001GB001662.

Campin, J. M., and H. Goosse (1999), Parameterization of density-driven downsloping flow for a coarse-resolution ocean model in z-coordinate, *Tellus, Ser. A*, *51*, 412–430.

Carr, A. S., M. D. Bateman, D. L. Roberts, C. V. Murray-Wallace, Z. Jacobs, and P. J. Holmes (2010), The last interglacial sea-level high stand on the southern Cape coastline of South Africa, *Quat. Res.*, *73*, 351–363, doi:10.1016/j.yqres.2009.08.006.

Conway, H., B. L. Hall, G. H. Denton, A. M. Gades, and E. D. Waddington (1999), Past and Future Grounding-Line Retreat of the West Antarctic Ice Sheet, *Science*, *286*, 280–283, doi:10.1126/science.286.5438.280.

Gent, P. R., J. Willebrand, T. J. Dougall, and J. C. McWilliams (1995), Parameterizing eddy-induced transports in ocean circulation models, *J. Phys. Oceanogr.*, *25*, 463–474, doi:10.1175/1520-0485(1995)025<0463:PEITTI>2.0.CO;2.

Goosse, H., and T. Fichefet (1999), Importance of ice-ocean interactions for the global ocean circulation: A model study, *J. Geophys. Res.*, *104*(C10), 23,337–23,355, doi:10.1029/1999JC900215.

Goosse, H., E. Deleersnijder, T. Fichefet, and M. H. England (1999), Sensitivity of a global coupled ocean-sea ice model to the parameterization of vertical mixing, *J. Geophys. Res.*, *104*(C6), 13,681–13,695, doi:10.1029/1999JC900099.

Goosse, H., et al. (2010), Description of the Earth system model of intermediate complexity LOVECLIM version 1.2, *Geosci. Model Dev.*, *3*, 309–390, doi:10.5194/gmdd-3-309-2010.

Hattermann, T., and A. Levermann (2010), Response of Southern Ocean circulation to global warming may enhance basal ice shelf melting around Antarctica, *Clim. Dyn.*, *35*(5), 741–756, doi:10.1007/s00382-009-0643-3.

Hearty, P. J., J. T. Hollin, A. C. Neumann, M. J. O'Leary, and M. McCulloch (2007), Global sea-level fluctuations during the Last Interglaciation (MIS 5e), *Quat. Sci. Rev.*, *26*, 2090–2112, doi:10.1016/j.quascirev.2007.06.019.

Hodell, D. A., K. A. Venz, C. D. Charles, and U. S. Ninnemann (2003), Pleistocene vertical carbon isotope and carbonate gradients in the South Atlantic sector of the Southern Ocean, *Geochem. Geophys. Geosyst.*, *4*(1), 1004, doi:10.1029/2002GC000367.

Ivchenko, V. O., V. B. Zalesny, M. R. Drinkwater, and J. Schröter (2006), A quick response of the equatorial ocean to Antarctic sea ice/salinity anomalies, *J. Geophys. Res.*, *111*, C10018, doi:10.1029/2005JC003061.

Jongma, J. I., E. Driesschaert, T. Fichefet, H. Goosse, and H. Renssen (2009), The effect of dynamic-thermodynamic icebergs on the Southern Ocean climate in a three-dimensional model, *Ocean Modell.*, *26*, 104–113.

Jouzel, J., et al. (2007), Orbital and millennial Antarctic climate variability over the past 800,000 years, *Science*, *317*, 793–796, doi:10.1126/science.1141038.

Kim, S. J., and T. J. Crowley (2000), Increased Pliocene North Atlantic Deep Water: Cause or consequence of Pliocene warming?, *Paleoceanography*, *15*, 451–455, doi:10.1029/1999PA000459.

Lim, G. H., J. R. Holton, and J. M. Wallace (1991), The structure of the ageostrophic wind field in baroclinic waves, *J. Atmos. Sci.*, *48*, 1733–1745, doi:10.1175/1520-0469(1991) 048<1733:TSOTAW>2.0.CO;2.

Lythe, M. B., D. G. Vaughan, and the BEDMAP Consortium (2001), BEDMAP: A new ice thickness and subglacial topographic model of Antarctica, *J. Geophys. Res.*, *106*, 11,335–11,351, doi:10.1029/2000JB900449.

Ma, H., L. Wu, and L. Chun (2010), Global teleconnections in response to freshening over the Antarctic Ocean, *J. Clim.*, doi:10.1175/2010JCLI3634.1, in press.

Menviel, L., A. Timmermann, A. Mouchet, and O. Timm (2008), Climate and marine carbon cycle response to changes in the strength of the southern hemispheric westerlies, *Paleoceanography*, *23*, PA4201, doi:10.1029/2008PA001604.

Mercer, J. H. (1978), Glacial development and temperature trends in the Antarctic and in South America, in *Antarctic Glacial History and World Paleoenvironments*, pp. 73–79, A. A. Balkema, Rotterdam, Netherlands.

Mouchet, A., and L. M. Francois (1996), Sensitivity of a Global Oceanic Carbon Cycle Model to the circulation and to the fate of organic matter: Preliminary results, *Phys. Chem. Earth*, *21*, 511–516, doi:10.1016/ S0079-1946(97)81150-0.

Naish, T., et al. (2009), Obliquity-paced Pliocene West Antarctic ice sheet oscillations, *Nature*, *458*, 322–328, doi:10.1038/ nature07867.

Ninnemann, U. S., and C. D. Charles (2002), Changes in the mode of Southern Ocean circulation over the last glacial cycle revealed by foraminiferal stable isotopic variability, *Earth Planet. Sci. Lett.*, *201*, 383–396, doi:10.1016/ S0012-821X(02)00708-2.

Oppenheimer, M. (1998), Global warming and the stability of the West Antarctic Ice Sheet, *Nature*, *393*, 325–332, doi:10.1038/30661.

Oppenheimer, M., and R. B. Alley (2004), The West Antarctic Ice Sheet and long term climate policy, *Clim. Change*, *64*, 1–10, doi:10.1023/B:CLIM.0000024792.06802.31.

Opsteegh, J. D., R. J. Haarsma, F. M. Selten, and A. Kattenberg (1998), ECBILT: A dynamic alternative to mixed boundary conditions in ocean models, *Tellus, Ser. A.*, *50*, 348–367.

Pagani, M., Z. Liu, J. LaRiviere, and A. C. Ravelo (2010), High Earth-system climate sensitivity determined from Pliocene carbon dioxide concentrations, *Nat. Geosci.*, *3*, 27–30, doi:10.1038/ngeo724.

Pahnke, K., and R. Zahn (2005), Southern Hemisphere water mass conversion linked with North Atlantic climate variability, *Science*, *307*, 1741–1746, doi:10.1126/science.1102163.

Payne, A. J., A. Vieli, A. P. Shepherd, D. J. Wingham, and E. Rignot (2004), Recent dramatic thinning of largest west antarctic ice stream triggered by oceans, *Geophys. Res. Lett.*, *31*, L23401, doi:10.1029/2004GL021284.

Pollard, D., and R. M. DeConto (2009), Modelling West Antarctic ice sheet growth and collapse through the past five million years, *Nature*, *458*, 329–332, doi:10.1038/nature07809.

Raymo, M. E., B. Grant, M. Horowitz, and G. H. Rau (1996), Mid-Pliocene warmth: Stronger greenhouse and stronger conveyor, *Mar. Micropaleontol.*, *27*, 313–326, doi:10.1016/0377-8398 (95)00048-8.

Renssen, H., H. Goosse, T. Fichefet, V. Brovkin, E. Driesschaert, and F. Wolk (2005), Simulating the Holocene climate evolution at northern high latitudes using a coupled atmosphere-sea ice-ocean-vegetation model, *Clim. Dyn.*, *24*, 23–43, doi:10.1007/s00382-004-0485-y.

Richardson, G., M. R. Wadley, K. J. Heywood, and D. P. Stevens (2005), Short-term climate response to a freshwater pulse in the Southern Ocean, *Geophys. Res. Lett.*, *32*, L03702, doi:10.1029/2004GL021586.

Rignot, E., and S. S. Jacobs (2002), Rapid bottom melting widespread near Antarctic Ice Sheet grounding lines, *Science*, *296*, 2020–2023, doi:10.1126/science.1070942.

Scherer, R. P., A. Aldahan, W. Tulaczyk, G. Possnert, H. Englehardt, and B. Kamb (1998), Pleistocene collapse of the West Antarctic Ice Sheet, *Science*, *281*, 82–85, doi:10.1126/science.281.5373.82.

Stocker, T. F., A. Timmermann, M. Renold, and O. Timm (2007), Effects of salt compensation on the climate model response in simulations of large changes of the Atlantic Meridional Overturning Circulation, *J. Clim.*, *20*, 5912–5928, doi:10.1175/2007JCLI1662.1.

Stouffer, R. J., D. Seidov, and B. J. Haupt (2007), Climate response to external sources of freshwater: North Atlantic versus the Southern Ocean, *J. Clim.*, *20*, 436–448, doi:10.1175/ JCLI4015.1.

Swingedouw, D., T. Fichefet, P. Huybrechts, H. Goosse, E. Driesschaert, and M.-F. Loutre (2008), Antarctic ice-sheet melting provides negative feedbacks on future climate warming, *Geophys. Res. Lett.*, *35*, L17705, doi:10.1029/ 2008GL034410.

Swingedouw, D., T. Fichefet, H. Goosse, and M.-F. Loutre (2009), Impact of transient freshwater releases in the Southern Ocean on the AMOC and climate, *Clim. Dyn.*, *33*, 365-381, doi:10.1007/s00382-008-0496-1.

Trevena, J., W. P. Sijp, and M. H. England (2008), Stability of Antarctic Bottom Water formation to freshwater fluxes and implications for global climate, *J. Clim.*, *21*, 3310–3326, doi:10.1175/2007JCLI2212.1.

Van Der Burgh, J., H. Visscher, D. Dilcher, and M. Kürschner (1993), Paleoatmospheric signatures in Neogene fossil leaves, *Science*, *260*, 1788–1790, doi:10.1126/science.260. 5115.1788.

Weaver, A. J., O. A. Saenko, P. U. Clark, and J. X. Mitrovica (2003), Meltwater pulse 1A from Antarctica as a trigger of the Bølling-Allerød warm interval, *Science*, *299*, 1709–1713, doi:10.1126/science.1081002.

Zhang, J. (2007), Increasing Antarctic sea ice under warming atmospheric and ocean conditions, *J. Clim.*, *20*, 2515–2529, doi:10.1175/ JCLI4136.1.

L. Menviel, Climate and Environmental Physics, Oeschger Centre for Climate Change Research, University of Bern, Sidlerstr. 5, CH-3012 Bern, Switzerland. (menviel@climate. unibe.ch)

A. Mouchet, Département AGO, Université de Liège, Alle du 6 Aot, 17 Bt. B5c, B-4000 Liège, Belgium.

O. E. Timm and A. Timmermann, IPRC, SOEST, University of Hawai'i, 2525 Correa Rd., Honolulu, HI 96822, USA.